

## Cosmological Parameter Determination from Counts of Galaxies

Silviu Podariu and Bharat Ratra

*Department of Physics, Kansas State University, Manhattan, KS 66506.*

### ABSTRACT

We study constraints that anticipated DEEP survey galaxy counts versus redshift data will place on cosmological model parameters in models with and without a constant or time-variable cosmological constant  $\Lambda$ . This data will result in fairly tight constraints on these parameters. For example, if all other parameters of a spatially-flat model with a constant  $\Lambda$  are known, the galaxy counts data should constrain the nonrelativistic matter density parameter  $\Omega_0$  to about 5% (10%, 1.5%) at  $1\sigma$  with neutral (worst case, best case) assumptions about data quality.

*Subject headings:* cosmological parameters—cosmology: observation—large-scale structure of the universe—galaxies: general

### 1. Introduction

Current observational data favors cosmogonies with a low  $\Omega_0$ . The simplest such cold dark matter models have either flat spatial hypersurfaces and a constant or time-variable cosmological “constant”  $\Lambda$  (see, e.g., Peebles 1984; Peebles & Ratra 1988, hereafter PR; Ratra et al. 1997; Sahni & Starobinsky 2000; Steinhardt 1999; Carroll 2001), or open spatial hypersurfaces and no  $\Lambda$  (see, e.g., Gott 1982, 1997; Ratra & Peebles 1994, 1995; Cole et al. 1997; Górski et al. 1998). For a constant  $\Lambda$  with density parameter  $\Omega_\Lambda$ , these models lie along the lines  $\Omega_0 + \Omega_\Lambda = 1$  and  $\Omega_\Lambda = 0$ , respectively, in the two-dimensional  $(\Omega_0, \Omega_\Lambda)$  parameter space. Models in this two-dimensional parameter space have either closed, flat, or open spatial hypersurfaces, depending on the values of  $\Omega_0$  and  $\Omega_\Lambda$ . In this paper we study the general two-dimensional model as well as the special one-dimensional cases.

We also study a spatially-flat model with a time-variable  $\Lambda$ . The only known consistent realization of this quintessence scenario is that based on a scalar field ( $\phi$ ) with a scalar field potential  $V(\phi)$  (Ratra & Peebles 1988). In this paper we focus on the favored model which at low redshift  $z$  has  $V(\phi) \propto \phi^{-\alpha}$ ,  $\alpha > 0$  (PR; Ratra & Peebles 1988).<sup>1</sup> A scalar field is mathematically

---

<sup>1</sup>For recent discussions of quintessence see, e.g., Weinberg (2000), Matos & Ureña-López (2001), Armendariz-

equivalent to a fluid with a time-dependent speed of sound (Ratra 1991), and with  $V(\phi) \propto \phi^{-\alpha}$ ,  $\alpha > 0$ , the  $\phi$  energy density behaves like a cosmological constant that decreases with time. In our analysis of this model here we do not make use of the time-independent equation of state fluid approximation to the model, since this leads to incorrect results (e.g., Podariu & Ratra 2000). Effective fluid realizations of quintessence with a time-dependent equation of state have also been studied. However, since such an equation of state is arbitrary, observational constraints on it are largely determined by how it is modelled. Scalar field realizations of quintessence are much more compelling, and only a handful of simple  $V(\phi)$ 's exhibit quintessence.

Cosmic microwave background anisotropy measurements have been used to discriminate between the flat and open models (see, e.g., Ratra et al. 1999; Rocha et al. 1999; Knox & Page 2000; Douspis et al. 2001; Podariu et al. 2001b; Netterfield et al. 2001; Pryke et al. 2001; Stompor et al. 2001), and favor the flat case. These observations have also been used to constrain quintessence models, see, e.g., Brax, Martin, & Riazuelo (2000), Amendola (2001), Balbi et al. (2001), Doran et al. (2001), González-Díaz (2001), and Schulz & White (2001).

The flat-constant- $\Lambda$  model seems to be in conflict with a number of observations, including: (1) analyses of the rate of gravitational lensing of quasars and radio sources by foreground galaxies (see, e.g., Falco, Kochanek, & Muñoz 1998); and (2) analyses of the number of large arcs formed by strong gravitational lensing by clusters (Bartelmann et al. 1998). A spatially-flat quintessence model can accommodate the first constraint. See Ratra & Quillen (1992), Frieman & Waga (1998), and Waga & Frieman (2000) for discussions of the scalar field quintessence case, and Zhu (2000), Cappi (2001), and Dev et al. (2001) for the fluid quintessence case.

Type Ia supernova (SN Ia) apparent magnitude versus redshift data favor the flat model (see, e.g., Riess et al. 1998, 2001; Perlmutter et al. 1999; Podariu & Ratra 2000; Gott et al. 2001). For SN Ia constraints on scalar field quintessence models see, e.g., Podariu & Ratra (2000), Waga & Frieman (2000), Gott et al. (2001), Wiltshire (2001), and Pavlov et al. (2001). Turner & Riess (2001) discuss the effective fluid quintessence case. Higher quality SN Ia data, such as that anticipated from the proposed SNAP space telescope<sup>2</sup>, will result in tighter constraints on cosmological parameters. See Podariu, Nugent, & Ratra (2001b, hereafter PNR) for a discussion of the scalar field quintessence case, and e.g., Maor, Brustein, & Steinhardt (2001), Chevallier & Polarski (2001), Barger & Marfatia (2001), Huterer & Turner (2000), Wang & Garnavich (2001), Goliath et al. (2001), and Weller & Albrecht (2001) for discussions of the effective fluid quintessence

---

Picon, Mukhanov, & Steinhardt (2001), McDonald (2001), de Ritis & Marino (2000), Kaganovich (2001), Bean & Magueijo (2000), Sen & Seshadri (2000), Nunes & Mimoso (2000), and Hebecker & Wetterich (2001). Inverse power law scalar field potentials appear in some high energy particle physics models (see, e.g., Rosati 2001; Brax, Martin, & Riazuelo 2001). Brane quintessence models have also been discussed by, e.g., Maeda (2000), Huey & Lidsey (2001), Albrecht et al. (2001), Brax & Davis (2001), and Majumdar (2001). However, it appears non-trivial for string/M theory to accommodate quintessence (see, e.g., Hellerman, Kaloper, & Susskind 2001; Fischler et al. 2001; Moffat 2001; Halyo 2001; Cline 2001).

<sup>2</sup><http://snap.lbl.gov/>

case.

Loh & Spillar (1986) applied the number counts versus redshift test (Peebles 1993, §13) to a set of galaxies with photometric redshifts. For the redshift range of this test, galaxies are assumed to be conserved and the shape of the luminosity function of these galaxies is assumed to not change. Newman & Davis (2000, hereafter ND) suggest that anticipated DEEP (Deep Extragalactic Evolutionary Probe)<sup>3</sup> survey data on the number of galaxies (halos), at fixed rotation speed<sup>4</sup>, as a function of redshift will be an ideal candidate for the number counts test.<sup>5</sup> ND examine constraints from anticipated DEEP data on the parameters of the general constant  $\Lambda$  two-dimensional ( $\Omega_0$ ,  $\Omega_\Lambda$ ) model. They as well as Maor et al. (2001) and Huterer & Turner (2000) also study constraints on effective fluid quintessence models.

In this paper we focus on how well anticipated DEEP data will constrain parameters of various cosmological models. More specifically, for the quintessence case, for reasons discussed above, we focus on the favored scalar field model with  $V(\phi) \propto \phi^{-\alpha}$ ,  $\alpha > 0$  (PR; Ratra & Peebles 1988) instead of the effective fluid models considered by ND, Maor et al. (2001), and Huterer & Turner (2000).

We want to determine how well anticipated DEEP data discriminates between different cosmological model parameter values. To do this we pick a model and a range of model-parameter values and compute the predicted count of objects per steradian and per unit redshift increment,  $dN/dz(z)$ , for a grid of model parameter values that span this range. Figure 1 shows examples of  $(H_0^3/n_0)dN/dz(z)$ 's (here  $H_0$  is the Hubble constant and  $n_0$  is the proper number density of objects at  $z = 0$ ) computed in the time-variable  $\Lambda$  model (PR).

We follow ND and assume that number counts data from DEEP will be combined to provide  $dN/dz(z)$ 's and errors on  $dN/dz(z)$ 's for 8 uniform bins in redshift between  $z = 0.7$  and  $z = 1.5$ . In each redshift bin the statistical and systematic errors are combined to give a  $dN/dz(z)$  error distribution with standard deviation  $\sigma(z)$ . ND consider 10,000 galaxies distributed in redshift as  $(1+z)^{-2}$ . The “best” case estimate of  $\sigma(z)$  assumes Poisson errors only (ND) and results in  $\sigma(z_i) = 2.40, 2.54, 2.67, 2.81, 2.95, 3.09, 3.22, 3.36$  % for bins centered at  $z_i = 0.75, 0.85, \dots, 1.45$ , respectively.<sup>6</sup> To account for the uncertainty due to evolution, Huterer & Turner (2000) consider “neutral” (“worst”) case estimates of  $\sigma(z)$  determined by adding 10% (20%) in quadrature to the best case  $\sigma(z_i)$  values.

To determine how well number counts data will discriminate between different sets of parameter

---

<sup>3</sup><http://deep.ucolick.org/>

<sup>4</sup>ND argue that at fixed rotation speed the abundance of halos is almost independent of cosmological model and may be calibrated using semianalytical or numerical models.

<sup>5</sup>Haiman, Mohr, & Holder (2001) discuss the prospects of using X-ray and Sunyaev-Zeldovich effect selected clusters for this test.

<sup>6</sup>Since even the last bin contains a large number of galaxies, about 890, the Poisson distribution is close to Gaussian.

values, we pick a fiducial set of parameter values which give  $dN_{\text{F}}/dz(z)$  and compute

$$N_{\sigma}(P) = \sqrt{\sum_{i=1}^8 \left( \frac{dN/dz(P, z_i) - dN_{\text{F}}/dz(z_i)}{\sigma(z_i)dN_{\text{F}}/dz(z_i)} \right)^2}, \quad (1)$$

where the sum runs over the 8 redshift bins and  $P$  represents the model parameters, for instance  $\Omega_0$  and  $\Omega_{\Lambda}$  in the general two-dimensional constant  $\Lambda$  case.  $N_{\sigma}(P)$  is the number of standard deviations the parameter set  $P$  lies away from that of the fiducial model.

Results are presented and discussed in §2 and we conclude in §3.

## 2. Results and Discussion

As a test of our method, we compute constraints for two models ND study, the  $\Omega_0 = 0.3$ ,  $\Omega_{\Lambda} = 0.7$  constant  $\Lambda$  spatially-flat model in the upper panel of their Fig. 3 and the  $\Omega_0 = 0.3$ , fluid equation of state parameter  $w = -1$  spatially-flat effective fluid quintessence model in the lower panel of their Fig. 3 (and Fig. 14 of Huterer & Turner 2000). In both cases our constraint contours are in very good agreement with those derived by ND (and by Huterer & Turner 2000).

Figure 2 illustrates the ability of anticipated DEEP data to constrain cosmological parameters ( $\Omega_0$  and  $\Omega_{\Lambda}$ ) for the general two-dimensional constant  $\Lambda$  case. The chosen fiducial model is spatially-flat with  $\Omega_0 = 0.28$  and  $\Omega_{\Lambda} = 0.72$ . As expected, the constraint contours are elliptical, indicating that one combination of the parameters is better constrained than the other orthogonal combination. DEEP data with neutral case errors will lead to interesting constraints on cosmological parameters. DEEP data with best case errors will result in tighter constraints than current SN Ia data (compare with Fig. 5 of Podariu & Ratra 2000) but will be slightly less constraining than anticipated worst case SNAP data (see Fig. 3 of PNR). Note however that the worst case SNAP data errors of PNR are the baseline SNAP mission errors.

ND note that the major axis of the anticipated DEEP data constraint contours is rotated slightly relative to that of the anticipated SNAP data contours (compare Fig. 2 here with Fig. 3 of PNR). If DEEP data systematic errors (largely due to evolution) can be reduced well below the Huterer & Turner (2000) estimates, then a combined analysis of anticipated DEEP and SNAP data will result in very tight constraints on cosmological parameters. If the DEEP data systematic errors remain as large as the Huterer & Turner (2000) estimates, then this data will be less constraining than SNAP data and the slight relative rotation of the major axes of the contours will result in DEEP data only slightly tightening the SNAP contours.

Figure 3 illustrates the ability of anticipated DEEP data to discriminate between a constant and a time-variable  $\Lambda$  in a spatially-flat model. The chosen fiducial model has  $\Omega_0 = 0.28$  and  $\alpha = 0$ , and is a constant  $\Lambda$  model with  $\Omega_{\Lambda} = 0.72$ . Again, as expected, the contours are elliptical. DEEP data with best case errors will lead to good discrimination, roughly comparable to what should be

achieved by anticipated worst case SNAP data (see Fig. 4 of PNR).

Figure 4 illustrates the ability of DEEP data to constrain  $\Omega_0$  and  $\alpha$  in the spatially-flat time-variable  $\Lambda$  model (PR). The chosen fiducial model has  $\Omega_0 = 0.2$  and  $\alpha = 4$ . Again, anticipated DEEP data with best case errors will result in tight constraints, roughly comparable to what should be achieved by anticipated worst case SNAP data (see Fig. 5 of PNR).

If other data (e.g., cosmic microwave background anisotropy, or weak-lensing, or SN Ia apparent magnitude measurements) pinned down some of the cosmological parameters, DEEP data would then provide tighter constraints on the remaining parameters. For example, Fig. 5 shows constraints from anticipated DEEP data on  $\Omega_0$  in a spatially-flat constant  $\Lambda$  model and in an open  $\Lambda = 0$  model. DEEP data will provide fairly restrictive constraints on  $\Omega_0$  in both cases. For instance, at  $3\sigma$ , in the spatially-flat model (with  $\Omega_0 = 0.3$  and  $\Omega_\Lambda = 0.7$ ) we find  $\Omega_0 = 0.3_{-0.04}^{+0.05}$ ,  $= 0.3_{-0.07}^{+0.11}$ , and  $= 0.3_{-0.01}^{+0.01}$  for neutral, worst, and best case errors, while in the open model (with  $\Omega_0 = 0.3$  and  $\Omega_\Lambda = 0$ ) we have  $\Omega_0 = 0.3_{-0.10}^{+0.12}$ ,  $= 0.3_{-0.18}^{+0.26}$ , and  $= 0.3_{-0.03}^{+0.03}$  for neutral, worst, and best case errors. As expected from the elliptical shape of the contours in Fig. 2, anticipated DEEP data will constrain  $\Omega_0$  more tightly in the flat case than in the open case.

Figure 6 shows DEEP data constraints on  $\Omega_0$  and  $\alpha$  in the spatially flat time-variable  $\Lambda$  model, if other data were to require that either  $\alpha = 4$  or  $\Omega_0 = 0.2$  (in a fiducial model with  $\Omega_0 = 0.2$  and  $\alpha = 4$ ). Anticipated DEEP data will provide fairly tight constraints on these parameters. For example, if  $\alpha = 4$  we find  $\Omega_0 = 0.2_{-0.05}^{+0.07}$ ,  $= 0.2_{-0.08}^{+0.15}$ , and  $= 0.2_{-0.01}^{+0.02}$  for neutral, worst, and best case errors, while if  $\Omega_0 = 0.2$  we have  $\alpha = 4_{-1.3}^{+2.2}$ ,  $= 4_{-2.1}^{(>4)}$ , and  $= 4_{-0.4}^{+0.5}$  for neutral, worst (here the upper limit lies outside the parameter range considered), and best case errors, all at  $3\sigma$ .

### 3. Conclusion

Galaxy number counts versus redshift data of the quality assumed here will lead to fairly tight constraints on cosmological parameters. For example, in a spatially-flat constant  $\Lambda$  model where all other parameters are known, anticipated DEEP data will determine  $\Omega_0$  to about  $\pm 5.1\%$ ,  $\pm 9.8\%$ , and  $\pm 1.4\%$  (for neutral, worst, and best case errors respectively) at  $1\sigma$ . The corresponding errors on  $\Omega_0$  for the open case are about  $\pm 12\%$ ,  $\pm 24\%$ , and  $\pm 3.4\%$ . For the time-variable  $\Lambda$  model, when  $\alpha$  is fixed,  $\Omega_0$  will be known to about  $\pm 9.2\%$ ,  $\pm 18\%$ , and  $\pm 2.6\%$ , respectively, while when  $\Omega_0$  is fixed,  $\alpha$  will be determined to about  $\pm 14\%$ ,  $\pm 27\%$ , and  $\pm 3.8\%$ . In agreement with ND, we find that anticipated DEEP data with best case errors will be roughly as constraining as anticipated SNAP data with worst case errors, i.e., SNAP baseline mission errors (see §4 of PNR).

We acknowledge useful discussions with M. Davis, D. Huterer, P. Mukherjee, and P. Nugent, and support from NSF CAREER grant AST-9875031.

## REFERENCES

- Albrecht, A., Burgess, C.P., Ravndal, F., & Skordis, C. 2001, hep-th/0105261
- Amendola, L. 2001, Phys. Rev. Lett., 86, 196
- Armendariz-Picon, C., Mukhanov, V., & Steinhardt, P.J. 2001, Phys. Rev. D, 63, 103510
- Balbi, A., Baccigalupi, C., Matarrese, S., Perrotta, F., & Vittorio, N. 2001, ApJ, 547, L89
- Barger, V., & Marfatia, D. 2001, Phys. Lett. B, 498, 67
- Bartelmann, M., Huss, A., Colberg, J.M., Jenkins, A., & Pearce, F.R. 1998, A&A, 330, 1
- Bean, R., & Magueijo, J. 2000, astro-ph/0007199
- Brax, P., & Davis, A.C. 2001, hep-th/0105269
- Brax, P., Martin, J., & Riazuelo, A. 2000, Phys. Rev. D, 62, 103505
- Brax, P., Martin, J., & Riazuelo, A. 2001, Phys. Rev. D, submitted
- Cappi, A. 2001, Astro. Lett. Comm., in press
- Carroll, S.M. 2001, Living Rev. Relativity, 4, 2001-1
- Chevallier, M. & Polarski, D. 2001, Int. J. Mod. Phys. D, 10, 213
- Cline, J.M. 2001, JHEP, submitted
- Cole, S., Weinberg, D.H., Frenk, C.S., & Ratra, B. 1997, MNRAS, 289, 37
- de Ritis, R., & Marino, A.A. 2000, Phys. Rev. Lett., submitted
- Dev, A., Jain, D., Panchapakesan, N., Mahajan, S., & Bhatia, V.B. 2001, astro-ph/0104076
- Doran, M., Lilley, M., Schwindt, J., & Wetterich, C., 2001, ApJ, in press
- Douspis, M., Bartlett, J.G., Blanchard, A., & Le Dour, M. 2001, A&A, 368, 1
- Falco, E.E., Kochanek, C.S., & Muñoz, J.A. 1998, ApJ, 494, 47
- Fischler, W., Kashani-Poor, A., McNees, R., & Paban, S. 2001, JHEP, submitted
- Frieman, J.A., & Waga, I. 1998, Phys. Rev. D, 57, 4642
- Goliath, M., Amanullah, R., Astier, P., Goobar, A., & Pain, R. 2001, A&A, submitted
- González-Díaz, P.F. 2001, astro-ph/0103194
- Górski, K.M., Ratra, B., Stompor, R., Sugiyama, N., & Banday, A.J. 1998, ApJS, 114, 1

- Gott, J.R. 1982, *Nature*, 295, 304
- Gott, J.R. 1997, in *Critical Dialogues in Cosmology*, ed. N. Turok (Singapore: World Scientific), 519
- Gott, J.R., Vogeley, M.S., Podariu, S., & Ratra, B. 2001, *ApJ*, 549, 1
- Haiman, Z., Mohr, J.J., & Holder, G.P. 2001, *ApJ*, 553, 545
- Halyo, E. 2001, hep-ph/0105216
- Hebecker, A., & Wetterich, C. 2001, *Phys. Lett. B*, 497, 281
- Hellerman, S., Kaloper, N. & Susskind, L. 2001, *JHEP*, 0106, 003
- Huey, G., & Lidsey, J.E. 2001, astro-ph/0104006
- Huterer, D., & Turner, M.S. 2000, *Phys. Rev. D*, submitted
- Kaganovich, A.B. 2001, *Phys. Rev. D*, 63, 025002
- Knox, L., & Page, L. 2000, *Phys. Rev. Lett.*, 85, 1366
- Loh, E.D., & Spillar, E.J. 1986, *ApJ*, 307, L1
- Maeda, K. 2000, astro-ph/0012313
- Majumdar, A.S. 2001, astro-ph/0105518
- Maor, I., Brustein, R., & Steinhardt, P.J. 2001, *Phys. Rev. Lett.*, 86, 6
- Matos, T., & Ureña-López, L.A. 2001, *Phys. Rev. D*, 63, 063506
- McDonald, J. 2001, *Phys. Lett. B*, 498, 263
- Moffat, J.W. 2001, hep-th/0105017
- Netterfield, C.B., et al. 2001, *ApJ*, submitted
- Newman, J.A., & Davis, M. 2000, *ApJ*, 534, L11 (ND)
- Nunes, A., & Mimoso, J.P. 2001, *Phys. Lett. B*, 488, 423
- Pavlov, M., Rubano, C., Sazhin, M., & Scudellaro, P. 2001, astro-ph/0106068
- Peebles, P.J.E. 1984, *ApJ*, 284, 439
- Peebles, P.J.E. 1993, *Principles of Physical Cosmology* (Princeton: Princeton University Press)
- Peebles, P.J.E., & Ratra, B. 1988, *ApJ*, 325, L17 (PR)

- Perlmutter, S., et al. 1999, *ApJ*, 517, 565
- Podariu, S., Nugent, P. & Ratra, B. 2001a, *ApJ*, 553, 1 (PNR)
- Podariu, S., & Ratra, B. 2000, *ApJ*, 532, 109
- Podariu, S., Souradeep, T., Gott, J.R., Ratra, B., & Vogeley, M.S. 2001b, *ApJ*, 559, in press, astro-ph/0102264
- Pryke, C., Halverson, N.W., Leitch, E.M., Kovac, J., Carlstrom, J.E., Holzzapfel, W.L., & Dragovan, M. 2001, *ApJ*, submitted
- Ratra, B. 1991, *Phys. Rev. D*, 43, 3802
- Ratra, B., & Peebles, P.J.E. 1988, *Phys. Rev. D*, 37, 3406
- Ratra, B., & Peebles, P.J.E. 1994, *ApJ*, 432, L5
- Ratra, B., & Peebles, P.J.E. 1995, *Phys. Rev. D*, 52, 1837
- Ratra, B., & Quillen, A. 1992, *MNRAS*, 259, 738
- Ratra, B., Stompor, R., Ganga, K., Rocha, G., Sugiyama, N., & Górski, K.M. 1999, *ApJ*, 517, 549
- Ratra, B., Sugiyama, N., Banday, A.J., & Górski, K.M. 1997, *ApJ*, 481, 22
- Riess, A.G., et al. 1998, *AJ*, 116, 1009
- Riess, A.G., et al. 2001, *ApJ*, in press
- Rocha, G., Stompor, R., Ganga, K., Ratra, B., Platt, S.R., Sugiyama, N., & Górski, K.M. 1999, *ApJ*, 525, 1
- Rosati, F. 2001, *Nucl. Phys. Proc. Supp.*, 95, 74
- Sahni, V., & Starobinsky, A. 2000, *Int. J. Mod. Phys. D*, 9, 373
- Schulz, A.E., & White, M. 2001, astro-ph/0104112
- Sen, S., & Seshadri, T.R. 2000, gr-qc/0007079
- Steinhardt, P.J. 1999, in *Proceedings of the Pritzker Symposium on the Status of Inflationary Cosmology*, in press
- Stompor, R., et al. 2001, *ApJ*, submitted
- Turner, M.S., & Riess, A.G. 2001, *ApJ*, submitted
- Waga, I., & Frieman, J.A. 2000, *Phys. Rev. D*, 62, 043521



Wang, Y., & Garnavich, P.M. 2001, ApJ, 552, 445

Weinberg, S. 2000, astro-ph/0005265

Weller, J., & Albrecht, A. 2001, astro-ph/0106079

Wiltshire, D.L. 2001, in *Cosmology and Particle Physics*, ed. J. García-Bellido, R. Durrer, & M. Shaposhnikov (New York: AIP), in press

Zhu, Z.-H. 2000, Mod. Phys. Lett. A, 15, 1023

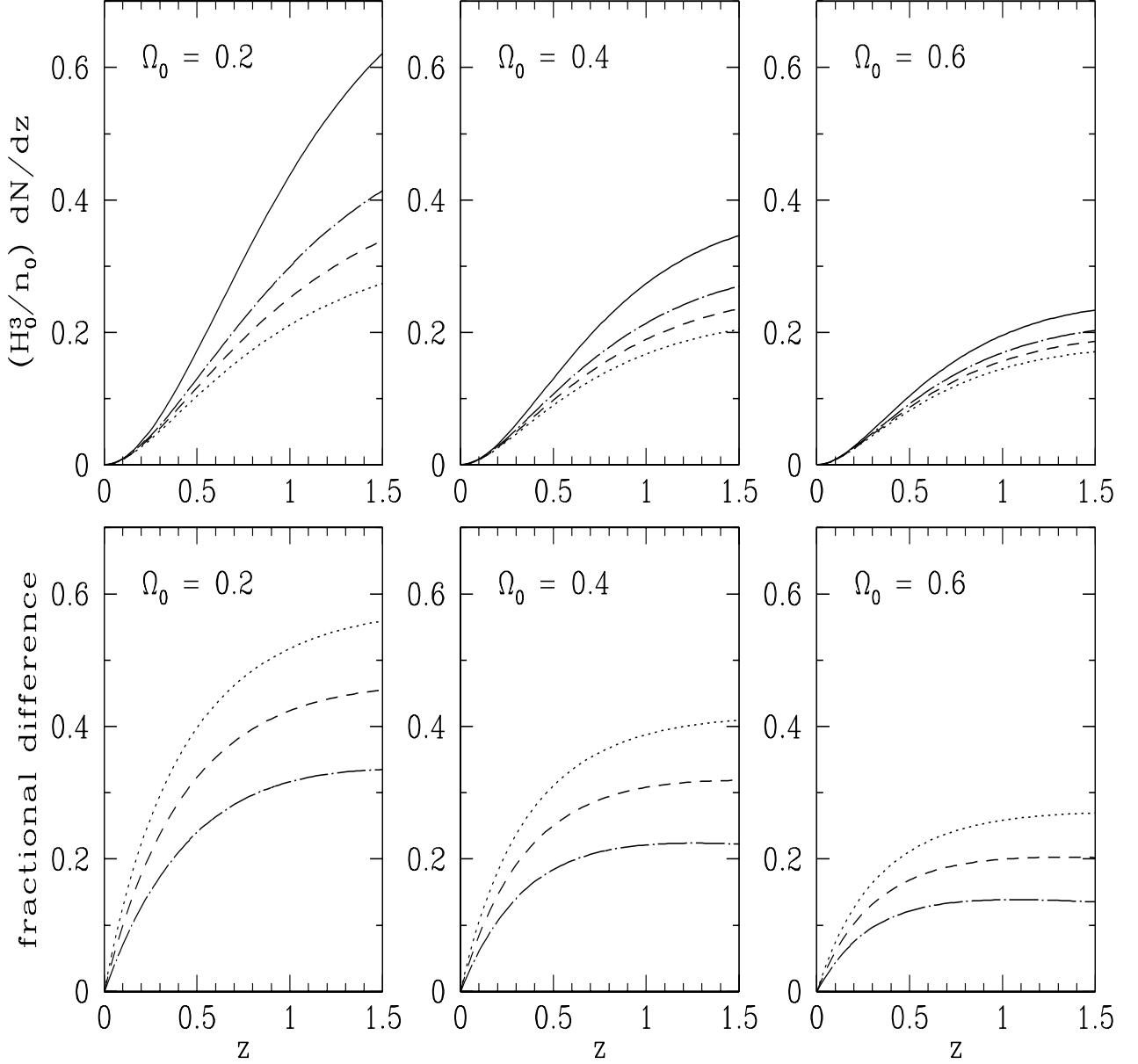


Fig. 1.— Lines in the panels in the upper row show normalized counts of objects per steradian and per unit redshift interval  $(H_0^3/n_0)dN/dz(z, \alpha)$  as a function of redshift  $z$  for various values of  $\alpha$  in the spatially-flat time-variable  $\Lambda$  model with scalar field potential  $V(\phi) \propto \phi^{-\alpha}$ . In descending order at  $z = 1.5$  the lines correspond to  $\alpha = 0, 2, 4,$  and  $8$  (solid, dot-dashed, dashed, and dotted curves respectively).  $\alpha = 0$  is the constant  $\Lambda$  model. From left to right the three panels correspond to  $\Omega_0 = 0.2, 0.4,$  and  $0.6$ . The three lower panels show the fractional differences relative to the  $\alpha = 0$  case,  $1 - [dN/dz(z, \alpha)]/[dN/dz(z, \alpha = 0)]$ , as a function of  $z$ , for the values of  $\Omega_0$  used in the upper panels. Here the lines correspond to  $\alpha = 8, 4,$  and  $2$ , in descending order at  $z = 1.5$ .

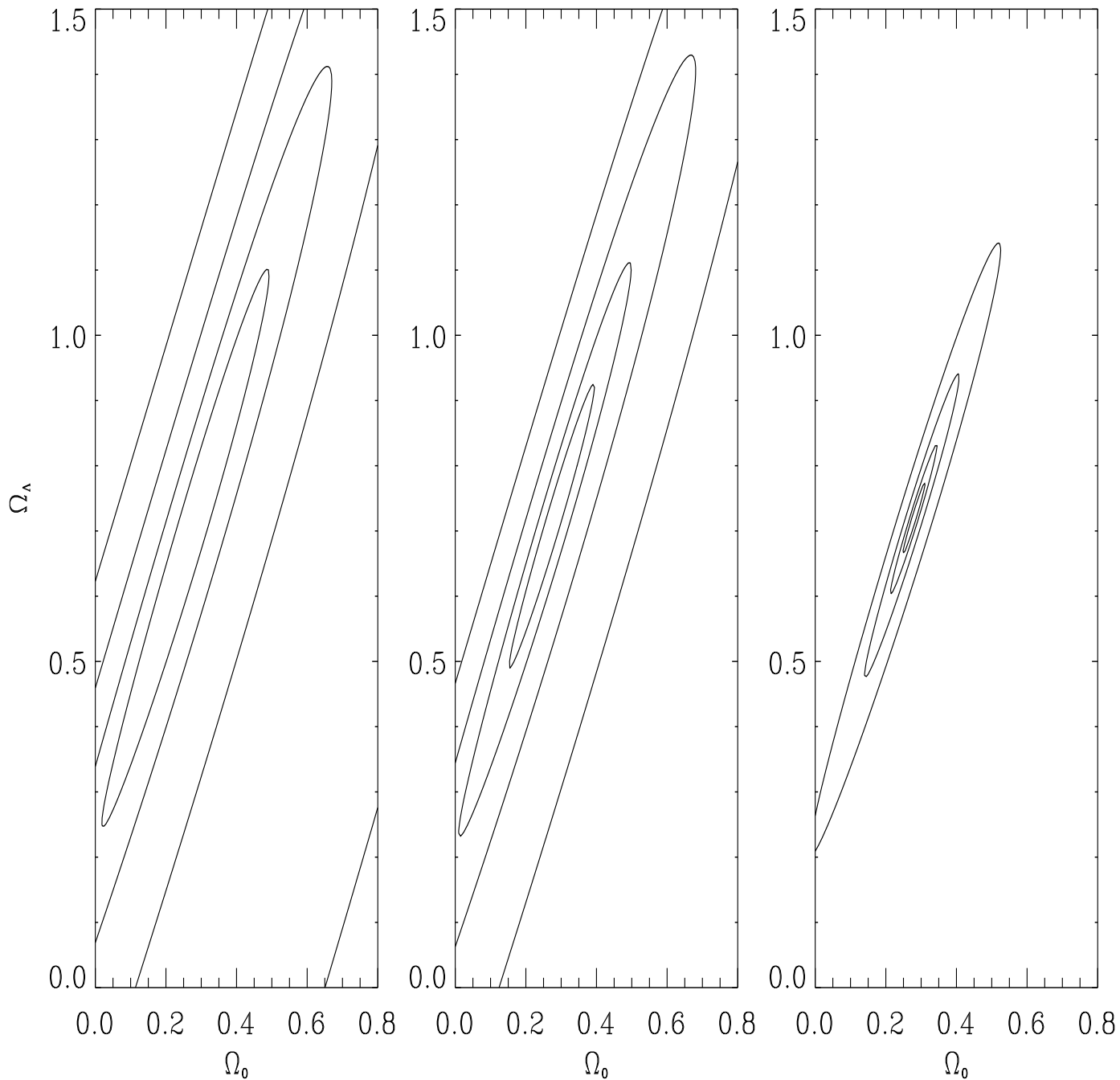


Fig. 2.— Contours of  $N_\sigma = 1, 2, 4$ , and  $8$  for the constant  $\Lambda$  model. Left panel is for anticipated DEEP data with worst case errors, center panel is for neutral case errors, and right panel is for best case errors. The fiducial model is spatially-flat with  $\Omega_0 = 0.28$  and  $\Omega_\Lambda = 0.72$ .

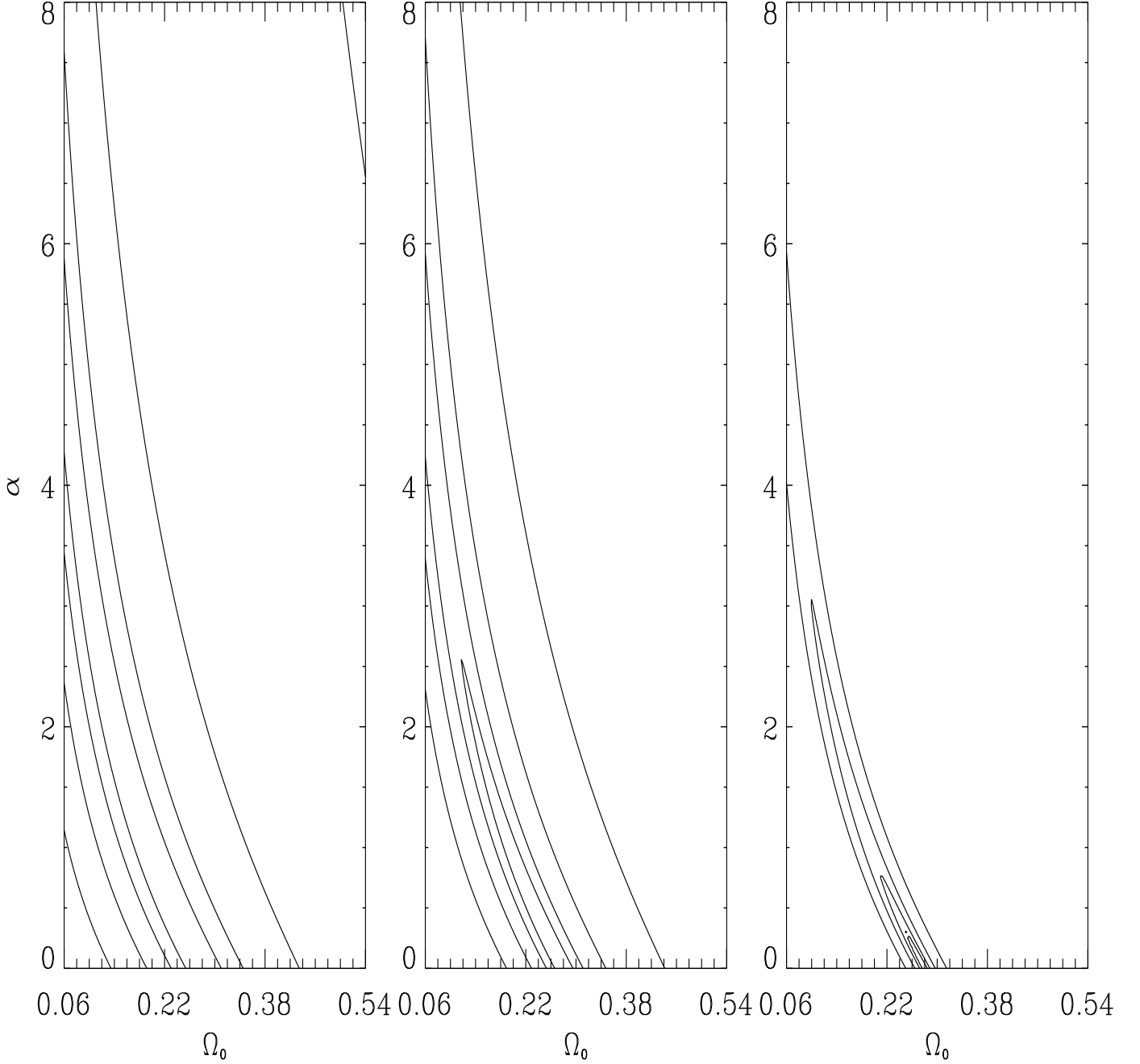


Fig. 3.— Contours of  $N_\sigma = 1, 2, 4,$  and  $8$  for the spatially-flat time-variable  $\Lambda$  model (PR). Left panel is for anticipated DEEP data with worst case errors, center panel is for neutral case errors, and right panel is for best case errors. The fiducial model has  $\Omega_0 = 0.28$  and  $\alpha = 0$  (and is thus a constant  $\Lambda$  model with  $\Omega_\Lambda = 0.72$ ; this is also the fiducial model used in Fig. 2).

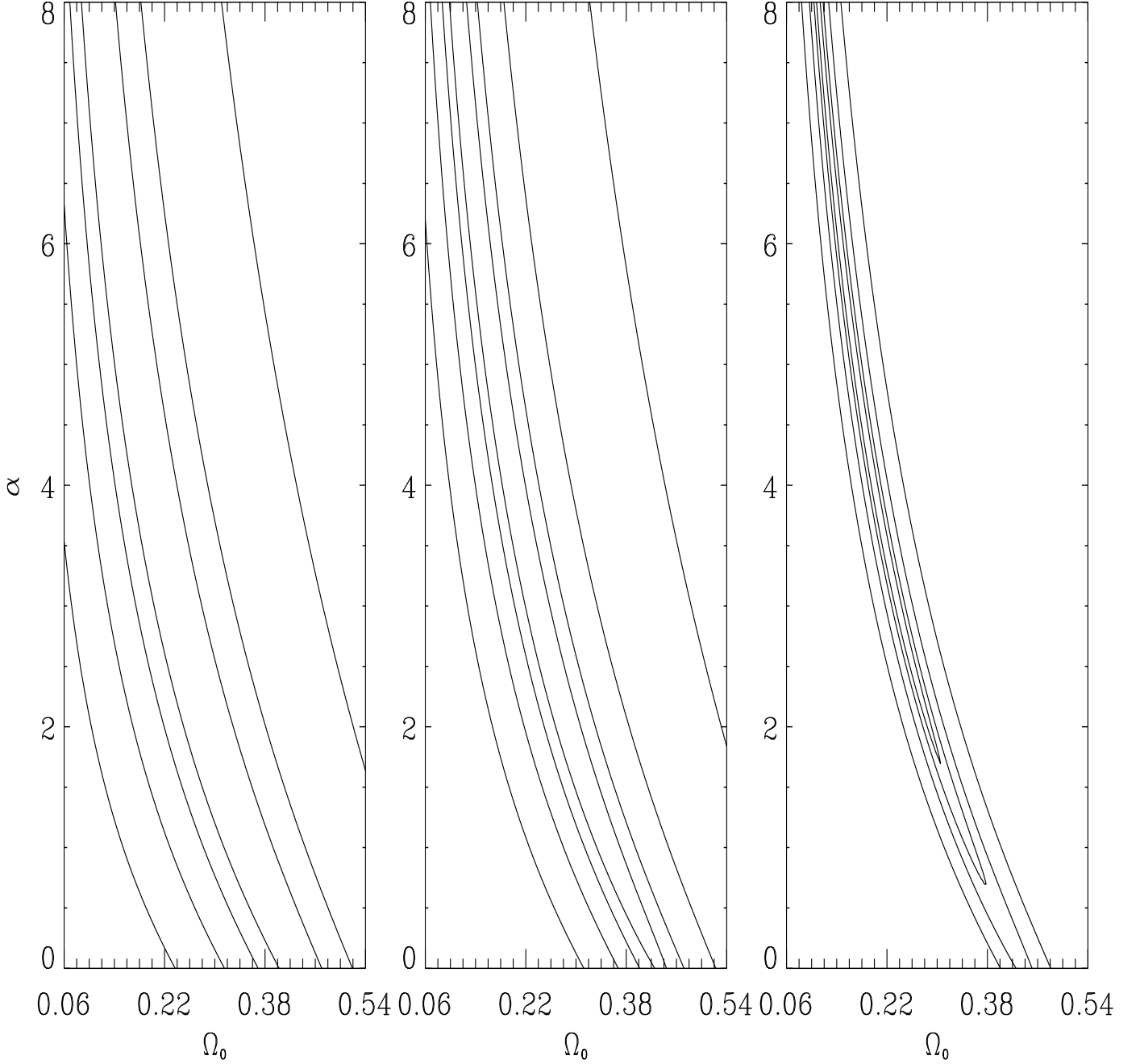


Fig. 4.— Contours of  $N_\sigma = 1, 2, 4$ , and  $8$  for the spatially-flat time-variable  $\Lambda$  model. Left panel is for anticipated DEEP data with worst case errors (part of the  $N_\sigma = 8$  contour lies to the top and right of the upper right hand corner of this panel), center panel is for neutral case errors, and right panel is for best case errors. The fiducial model has  $\Omega_0 = 0.2$  and  $\alpha = 4$ .

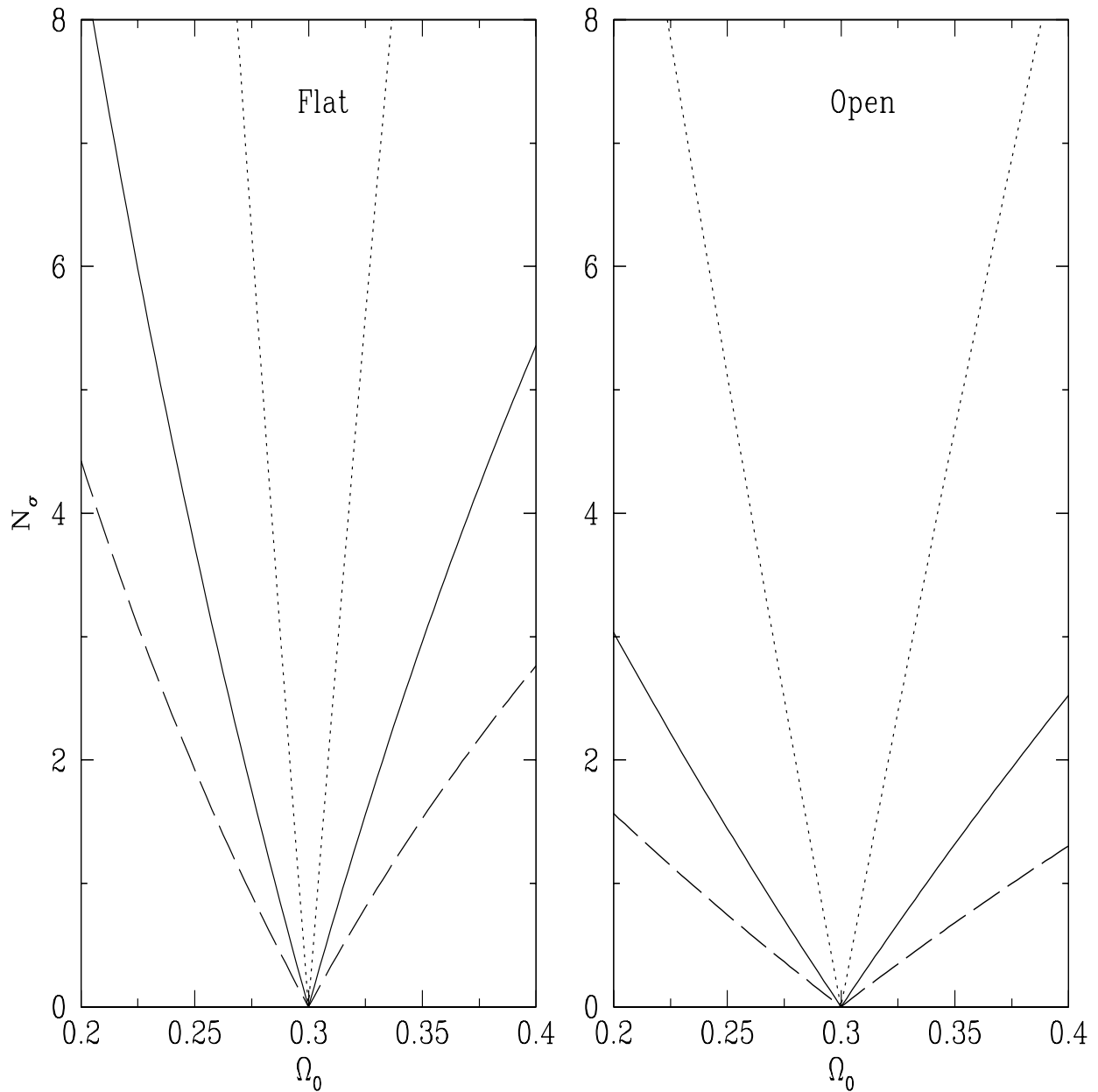


Fig. 5.—  $N_\sigma(\Omega_0)$  for a flat model with a constant  $\Lambda$  (left panel) and for an open model with no  $\Lambda$  (right panel). In both cases the fiducial model has  $\Omega_0 = 0.3$ , with  $\Omega_\Lambda = 0.7$  and 0, respectively. Solid lines are for neutral case DEEP errors while dotted (dashed) lines are for best (worst) case ones.

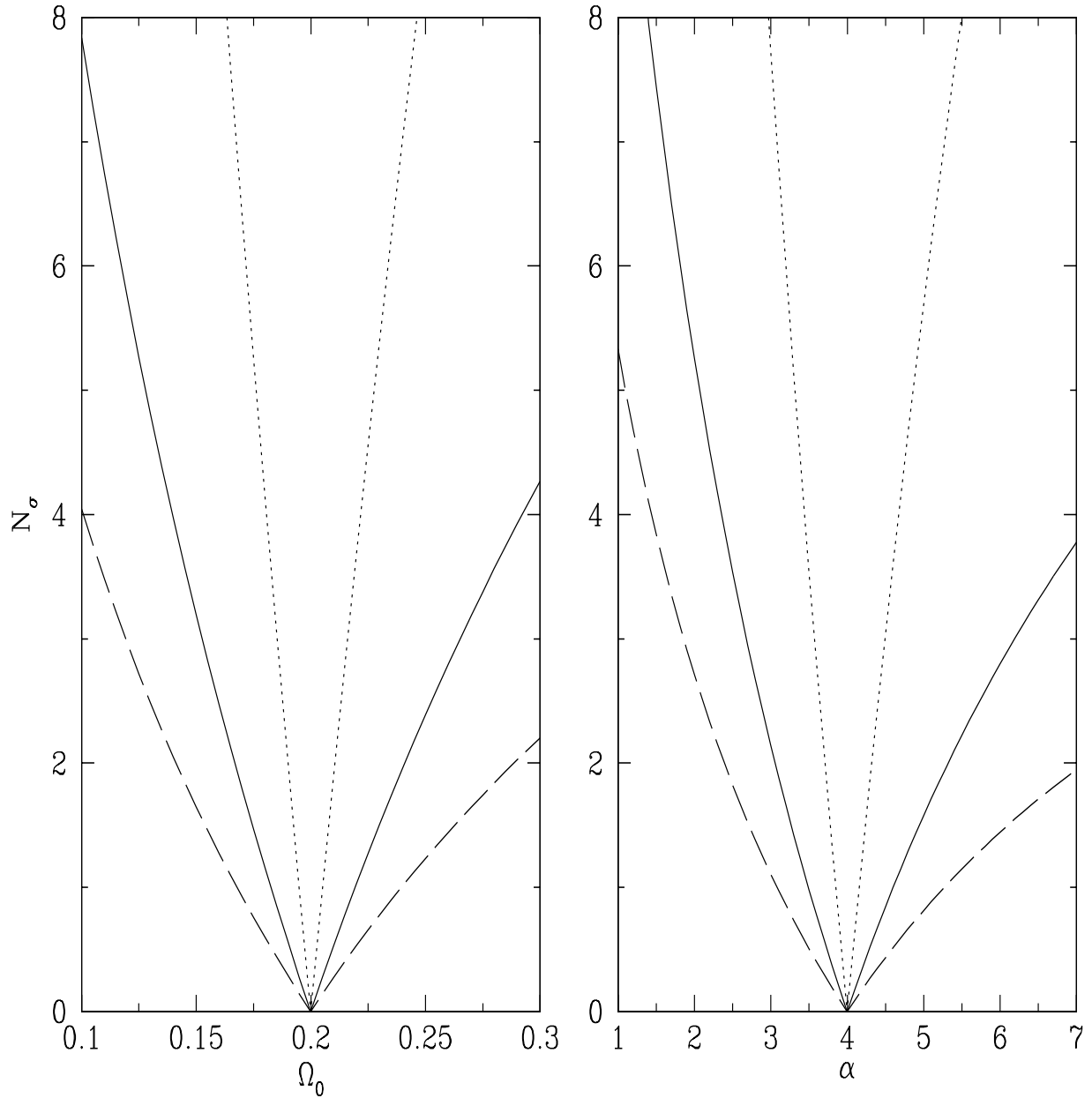


Fig. 6.—  $N_\sigma(\Omega_0)$  (left panel) and  $N_\sigma(\alpha)$  (right panel) for the spatially-flat time-variable  $\Lambda$  model (PR). In both cases the fiducial model has  $\Omega_0 = 0.2$  and  $\alpha = 4$ . Solid lines are for neutral case DEEP errors while dotted (dashed) lines are for best (worst) case ones.